ACS OMEGA

Open Access



http://pubs.acs.org/journal/acsodf

Article

# Orange Mesocarp Extract as a Natural Surfactant: Impact on Fluid−Fluid and Fluid−Rock Interactions during Chemical Flooding

Amalate Ann Obuebite,* Obumneme Onyeka Okwonna, William Iheanyi Eke, and Onyewuchi Akaranta

Cite This: *ACS Omega* 2024, 9, 4263−4276

Read Online

ACCESS | Metrics & More | Article Recommendations

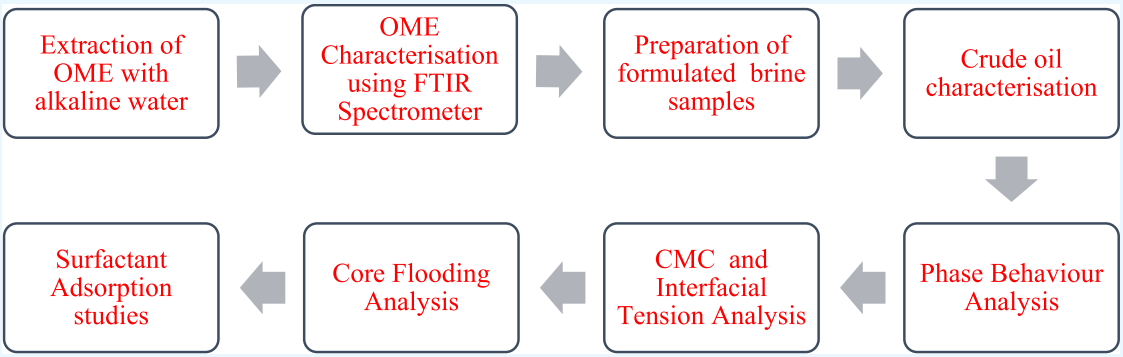


**ABSTRACT:** Surfactant flooding has suffered a huge setback owing to its cost and the ecotoxic nature of synthetic surfactants. The potential of natural surfactants for enhanced oil recovery has attracted a great deal of research interest in recent times. In this research, orange mesocarp extract (OME) was studied as a potential green surface-active agent in recovering heavy oil. The extract obtained from the orange (*Citrus sinensis*) mesocarp using alkaline water as solvent was characterized by Fourier transform infrared spectrophotometry . Phase behavior was studied to ascertain its stability at 100 °C and compatibility with divalent ions. Microemulsion system, interfacial tension, optimal salinity, and critical micelle concentration were analyzed to evaluate the surfactant. Oil displacement analysis using an oil−wet sandstone medium under reservoir conditions was performed. Surfactant adsorption mechanism on the core was investigated at atmospheric conditions (28 °C) using the Langmuir, Freundlich, Temkin, and linear isotherm models, while the kinetics pattern was modeled with the pseudo-first-order, pseudo-second-order, intraparticle diffusion, and Elovich models. Results showed fluid compatibility and bicontinuous microemulsion at varied temperatures. Surfactant flooding produced an additional oil recovery of 44 and 29.1%, which confirms the capability of this natural surfactant in recovering heavy oil. Langmuir isotherm gave the highest correlation coefficient ($R^2$) value of 0.982, indicating that the adsorption of the surfactant (OME) on the core occurred at specific homogeneous sites, which when occupied by a higher surfactant concentration will disallow further adsorption on these sites. From the $R^2$ values, almost all of the kinetic models corroborated good adsorption capacity of the core and an affinity for the surfactant at low concentration. This indicates that low concentration of the surfactant may not favor the enhanced oil recovery operation due to adsorption in the reservoirs, hence the need to flood at a higher surfactant concentration.



## 1. INTRODUCTION

Despite the global concern of fossil fuels contributing greatly to climate change and the efforts on energy transition to cleaner, renewable, and more environmentally friendly energy sources, the demand for fossil fuels will still be prevalent until the year 2050.[1] With an increasing global energy demand comes the need to increase hydrocarbon production from oil reservoirs. Since April 2022, Nigeria, a member of the organization of petroleum exporting countries (OPEC) has experienced a steady decline in oil production and an inability to meet the production quota allotted by OPEC. The economic dependence of Nigeria and other oil-producing countries on the proceeds from the sale of hydrocarbons reiterates the importance of increasing or optimizing oil recovery from proven hydrocarbon reserves at minimal cost. Chemical enhanced oil recovery (CEOR) describes processes that involve the use of chemicals such as surfactants, alkali, and polymers in oil recovery with the aim of increasing the capillary number which in turn reduces the interfacial tension (IFT)

Received: June 29, 2023
Revised: December 5, 2023
Accepted: December 20, 2023
Published: January 12, 2024

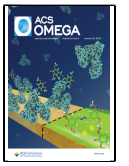

values between oil and brine, reducing the mobility ratio, gathering the residual oil, and increasing the sweep efficiency. Effective use of these chemicals is subject to certain inherent attributes of the reservoir such as reservoir type and depth and concentration and salinity of the formation brine.[2] In surfactant flooding, surface-active agents are used to reduce the IFT between two phases while also altering the wettability of the reservoir rock.[3] Some successful field applications of surfactant flooding include Tanjing field in Indonesia, Bentiu field in South Sudan, and Yates field in Texas (USA), which resulted in enhanced oil recovery as well as reduced IFT.[4−7] The synergy in the alkali−surfactant system as reported by Sheng[8] produced an ultra-low IFT value compared to that produced using either alkali or surfactant singly. Previous studies have shown the effect of organic acid inherent in the oil on the IFT reduction especially in a surfactant−oil system.[9] In other words, low acid concentration in such a system will increase the IFT and vice versa, while the addition of alcohol could also have an impact on the IFT. Liu et al.[10] only observed an emulsified heavy oil when an aqueous solution of alkali and surfactant was used, thus reporting a higher oil recovery when using the combined aqueous solution due to the synergistic effect of alkali and surfactant.

Despite these successful field cases, the high cost of these synthetic chemicals (which translates to increased operating cost and lower profit margin for oil-producing companies) and their negative environmental impact have greatly limited their application. Furthermore, the high adsorption rate and the susceptibility of these synthetic surfactants to high temperature and high-salinity reservoirs with hard brine have remained a challenge.[11] This is because surfactant adsorption increases significantly when brines containing divalent ions are used, resulting in a low surfactant performance. This is due to the electrostatic forces between the charges of the rock minerals and those of the surfactant.[12] Sandstone reservoirs comprising predominantly detrital clasts accounts for over 60% of the world's crude oil reservoirs and an annual oil production of about 22 billion barrels.[8] These sandstone reservoirs contain divalent ions, but conventional surfactant flooding requires formation brine devoid of these ions which is rare; thus, an expensive option of brine softening is proposed. However, factors such as site location make the process often impracticable. Most recovery mechanisms have been conducted in reservoirs with low salinity;[8] however, for high-salinity reservoirs, scale formation and chemical consumption occur due to the interaction of these chemicals with divalent ions, which impedes additional oil recovery.

Interestingly, recent studies[13−21] reported the efficiency of certain natural products obtained from plant and animal sources (biobased surfactants) as preferred alternatives to conventional synthetic surfactants. Saponin-rich plant sources have been widely used due to their foaming ability.[22,23] Saponins are among the most abundant plant-based products and belong to the group of nonionic surfactants, which are mostly used as cosurfactants due to their high resistance to salinity and their capacity to improve surfactant−brine−oil phase behavior.[24] Conversely, flavonoids are one of the most important group of plant-based natural compounds having phenolic structures.[25] Flavonoids have a low molecular weight and high solubility in nonpolar solvents such as methanol and are effective in chelating metal ions. Their application has been recorded in several industries ranging from food, pharmaceutical, health, and cosmetic industries due to the variety of biological properties they possess.[26] Recently, research interest in the application of flavonoids as oil field chemicals, such as natural surfactants with the IFT-reducing ability,[27,28] oil-in-water emulsion stabilizer,[29] drilling mud,[30] and ion exchangers,[31] has increased. The effectiveness of flavonoids in emulsion stabilization was reported by Luo et al.[32] as being highly dependent on pH. Obuebite et al.[33] in their experimental study of natural surfactants also noted that natural surfactants are less susceptible to high temperatures and brine containing divalent ions. The use of natural surfactants is rapidly gaining interest in the petroleum industry due to their ability to relatively modify surface in liquid systems[34] as well as their low cost, low toxicity, biodegradability, and availability.

Orange (*Citrus sinensis*) fruit is an agricultural produce that is commonly found in most parts of the world. The annual global orange production is reported to be over 50 million tonnes.[35] *C. sinensis* fruits are layered as exocarp, mesocarp, and endocarp. The only edible part of the orange is the endocarp, or the pulp filled with juice vesicles, while the exocarp and mesocarp are considered as waste. The exocarp is the outermost peel which is underlined by a mesocarp which is a sponge-like layer made up of various pore spaces and connected colorless cells, occurring close to the peel. Oranges are locally abundant in Nigeria, and its mesocarp constitutes a large portion of the waste biomass. The potential to transform waste to a an economically valuable resource and reduce negative environmental imprints is an added advantage to research. The phytochemical composition of the orange mesocarp reveals that they contain a high amount of flavonoids (rutin), phenolic acids, glycoside, saponins, organic acids, steroids, esters, alcohols, and alkaloids and a high moisture content which promotes microbial growth.[36] Due to the antioxidant, anti-inflammatory, and antibacterial properties of orange waste, they find good use in the food, medical, and pharmaceutical industries. However, despite the phytochemical composition, which suggests that they may have some foaming qualities, they have not been evaluated as possible natural surfactants.

Furthermore, studying the adsorption mechanism of natural surfactants is crucial in determining their suitability. The use of the surfactants for EOR is favored by their capacity to reduce IFT between the oil and water phases. Adsorption loss is a major challenge in surfactant flooding for EOR because when surfactants are lost via adsorption in the reservoir rock during surfactant flooding, it affects their effectiveness and performance in reducing the IFT between the oil and water phases, with resultant technical and economic implications. To this end, the adsorption of the natural surfactant on the sandstone core was investigated using a model of the adsorption isotherms and kinetics of the process. The aim of this study was to investigate the effectiveness of the orange mesocarp extract (OME) as a natural surfactant in recovering residual oil in heavy oil sandstone reservoirs containing divalent ions and determine the mechanism and kinetics of its adsorption on the sandstone core. This study is novel and will go a long way in underscoring the use of this natural surfactant for EOR operation in addition to other benefits such as biodegradability, availability, low cost, and environmental friendliness unlike the commercial industrial surfactants.


https://doi.org/10.1021/acsomega.3c04651
ACS Omega 2024, 9, 4263−4276

## 2. MATERIALS AND METHODS

**2.1. Materials.** Oranges were sourced from a local market (4.8472°N, 6.9746°E) in the Obio-Akpor LGA, Rivest State, Nigeria. Reagents used include Analar grade sodium hydroxide, sodium chloride, calcium chloride, magnesium chloride, and distilled water. The core sample was sourced from a sandstone reservoir from Agbada formation, with the sandstone core sample comprising quartz and clay minerals such as muscovite and kaolinite.

Some of the equipment/apparatus used in carrying out the research include gas chromatography−mass spectrometry (GC−MS), Fourier transform infrared (FTIR) spectrometer, rotary evaporator, conductivity meter, pH meter, water bath, core flooding equipment, and glassware (funnels, beakers, glass tubes, and pipettes).

**2.2. Methods.** The study was conducted in the following sequence: biomass/agrowaste preparation, natural product extraction, sample characterization, brine preparation, critical micelle concentration (CMC) determination, IFT determination, and phase behavior, core flooding, and adsorption studies.

**2.3. Preparation of Biomass and Brine.** Orange mesocarp was peeled off, sun-dried, and pulverized. The sample was stored in an airtight plastic bag before extraction. Synthetic brine samples were simulated to reflect actual formation brine. For soft brine solution, sodium chloride and potassium chloride of varied concentrations with a total dissolved solid (TDS) of 30,000 ppm and 3% salinity were used, while the hard brine had two additional salts introduced, namely, calcium chloride and magnesium chloride with similar TDS of which 4000 ppm accounts for the divalent ions $Ca^{2+}$ and $Mg^{2+}$. The composition of both brines is outlined Table 1), and the brines were prepared as detailed by Bolaji et al.[37]

**Table 1. Composition of the Formulated Brine**

| | concentration (ppm) | |
|---|---|---|
| component | hard brine | soft brine |
| NaCl | 23,000 | 23,000 |
| KCl | 7000 | 2000 |
| $MgCl_2$ | | 2000 |
| $CaCl_2$ | | 3000 |
| total dissolved solid | 30,000 | 30,000 |

Furthermore, the pH, density, and viscosity of both brine solutions were evaluated at 25 and 80 °C depicting ambient and reservoir temperatures, respectively.

**2.4. Biomass Extraction.** The extraction of orange mesocarp was conducted using 1% sodium hydroxide solution as the solvent at ambient temperature. The solvent was prepared by dissolving 10 g of NaOH in 1 L of distilled water. The powdered orange mesocarp was allowed to soak for 12 h in the sodium hydroxide solution with intermittent agitation. The solvent was removed from the filtrate using a rotary evaporator, and the resultant concentrated extract was packaged and labeled "OME". The spectrum of the OME was recorded using a Fourier transform infrared spectrophotometer.

**2.5. Critical Micelle Concentration.** CMC was determined by the electrical conductivity method. The electrical conductivity of the extract solution was measured at different concentrations. CMC was obtained as the point of inflection on the plot of the conductivity against the surfactant concentration.

**2.6. Crude Oil Characterization.** Dead oil from the Niger Delta basin was used in this study and characterized using its viscosity, specific gravity, American Petroleum Institute (API) gravity, and total acid number (TAN). A rheometer was used to measure the dynamic viscosity of the oil, while the specific gravity was measured using the ASTM D287 standard test method. Using the potentiometric titration technique, the measure of acidity in the oil was evaluated and computed afterward into eqs 1 and 2.

$$\text{KOH vol (mol/L)} = \frac{(\text{KHP solution·grams}) \times (\text{KHP concentration})}{\text{KOH concentration}} \quad (1)$$

$$\text{Acid number} = (A - B) \times M \times \frac{56.1}{W} \quad (2)$$

where $A$ = volume of KOH solution used in the titration to the last inflection end point, mL, $B$ = volume corresponding to $A$ for blank titration, mL, $M$ = KOH concentration, mol/L, and $W$ = mass of oil sample, grams.

The API gravity was evaluated using the correlation of eq 3

$$\text{API} = [141.5/\text{SG}] - 131.5 \quad (3)$$

where SG = specific gravity.

**2.7. IFT Measurement.** The surface activities of OME as a natural surfactant were investigated using a surface interfacial tensiometer BZY-102. The IFT was investigated from a setup comprising a crude oil, surfactant, and brine solution. The effect of using different concentrations of the surfactant on the IFT of the oleic−aqueous system was observed and recorded. Brine composition was varied on the oil−brine system at constant surfactant concentration to ascertain the response of the various salts to IFT. Brines of NaCl, KCl, $CaCl_2$, and $MgCl_2$ with their equivalent concentrations were used. These tests were carried out at 25 and 80 °C.

**2.8. Compatibility Test.** A compatibility test was performed to determine fluid−fluid compatibility under varying concentrations. Hence, incompatibility was indicated by nonhomogeneity observed through precipitation and cloudiness. Different OME concentrations (0.5, 1.0, and 2.0%) were placed in various airtight glass containers each containing soft brine at a fixed salinity and volume. The setup was vigorously agitated to ensure homogeneity, while the setup was observed for 7 days. Only clear, cloudless samples were considered, while others that failed to meet this criterion were screened out. This process was repeated on the natural surfactant using hard brine. These tests were carried out at 25 and 80 °C.

**2.9. Salinity Scan Test.** The level of salinity tolerance of the OME in both brines under varied electrolyte concentrations was analyzed. The tests were conducted in test tubes, each containing 10 mL of the solution. With a constant OME micelle concentration, the salinity of the brine was altered as well as their pH value. The salinity range was determined using eq 4

$$C_1V_1 = C_2V_2 \quad (4)$$

**2.10. Phase Separation (Pipet) Test.** Phase separation (pipet) tests were also carried out to determine the interaction between the compatible aqueous phase and the oleic phase and



https://doi.org/10.1021/acsomega.3c04651
ACS Omega 2024, 9, 4263−4276

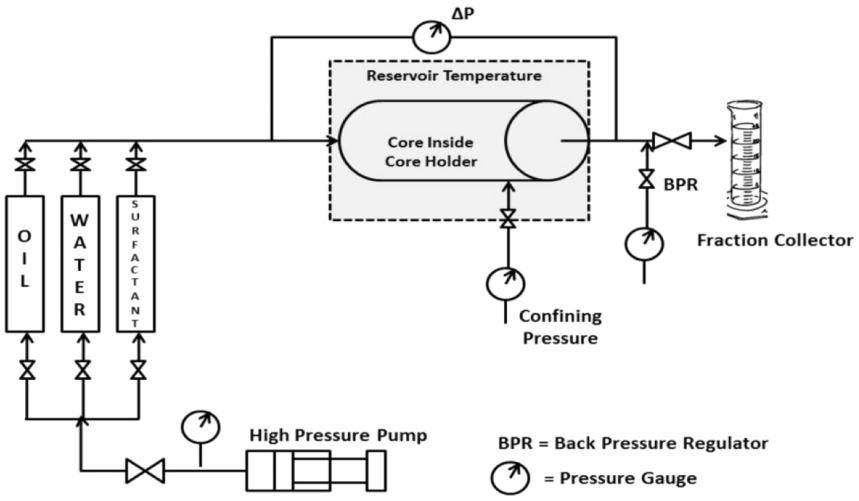


**Figure 1.** Core flooding setup.

ascertain the presence and type of microemulsion formed. The surfactant−brine solution and crude oil were added at equal volumes into different pipettes and sealed, and the different phase interfaces were recorded. The fluids were properly mixed and observed at a range of temperatures for 21 days. Solutions wherein bicontinuous microemulsion (suggestive of ultralow IFT) had formed were selected, and the level readings of the different phases were noted. The brine optimum salinity was determined via a plot of salinity as a variation of oil and water solubilization ratio.

**2.11. Oil Displacement Test.** Properties of the porous medium such as porosity and pore volume were determined, and the oil displacement performance of the OME serving as the surfactant agent was conducted under reservoir conditions of 80 °C and 8000 psi confining pressure using a sandstone core plug. The simplified sketch of the core flooding scheme is shown in Figure 1. The optimum salinity value of the brine and the CMC of the surfactant were used during the displacement test, and the additional recovery facilitated by surfactant flooding was computed.

The brine-saturated sandstone core was placed inside a pressurized core holder, and crude oil at 0.3 mL/min was used to completely displace brine and saturate the core to simulate a reservoir saturated with hydrocarbon. The displaced brine volume was read as the original oil in place (OOIP), while initial oil and irreducible water saturations were evaluated. Thereafter, 8.5 PV of brine at optimal salinity was injected into the core at an injection rate of 0.1 mL/min, thereby displacing oil to residual oil saturation. Two PV of the OME in soft brine at 0.1 mL/min was injected to enhance recovery of the residual oil left behind or bypassed during brine flooding. A similar test was carried out using hard brine at the same injection rate. The process was terminated when an oil cut of about 2% was observed.

**2.12. Adsorption Test.** The crushed core sample comprising quartz and minute traces of clay minerals (muscovite, illite, and kaolinite) served as the adsorbent. In preparing the adsorbent, the core was pulverized into a particle size range of 150−170 $\mu$m determined using a standard sieve.

**2.13. Preparation of the Surfactant Solution.** The OME natural surfactant solution was prepared by dissolving 0.10−8 g of the OME extract in 100 mL of distilled water to obtain solutions of a concentration range of 1000−80,000 mg/L, respectively.

**2.14. Adsorption Experiment.** Weighted amount of the natural surfactant (OME) of initial concentration range of 1000−80,000 ppm was used to attain equilibrium condition with the crushed sandstone core. Also, 8 g of the crushed core sample was added to 40 mL solution of the natural surfactant (OME) solution amidst vigorous agitation under constant room temperature of 28 °C. The conductivity of the surfactant solution was used to evaluate the surfactant concentration before and after the adsorption experiment with the crushed sandstone core sample. The concentration values were thereafter fitted into the theoretical model from where the adsorption ($q$) of the natural surfactant (OME) was obtained using the correlation of eq 5.

$$q = \frac{(C_0 - C_f) \times m_b}{m_c} \times 10^{-3} \tag{5}$$

where $q$ = amount of the surfactant adsorbed on the core surface (mg/g), $C_0$ = initial concentration of the surfactant solution before equilibration with the core sample (ppm), $C_f$ = final concentration of the surfactant solution after equilibration with the core sample (ppm), $m_b$ = total mass of solution in original bulk solution (g), and $m_c$ = total mass of the crushed core sample (g).

**2.15. Adsorption Models.** The relationship between the equilibrium concentration of the natural surfactants (OME) and the quantity of the adsorbate at constant temperature was modeled using the Langmuir, Freundlich, Temkin, and linear isotherm models.

*2.15.1. Langmuir Isotherm.* This isotherm applies to monolayer adsorption on homogeneous sites. In other words, this model assumes that adsorption takes place on specific homogeneous sites of the core sample, which when occupied by other adsorbates cannot allow further adsorption on these sites. The Langmuir isotherm is given by eq 6

$$q_e = \frac{q_0 K_{ad} C_e}{1 + K_{ad} C_e} \tag{6}$$

where $q_e$ = adsorption capacity of the core sample at equilibrium, $C_e$ = surfactant concentration at equilibrium, $K_{ad}$


https://doi.org/10.1021/acsomega.3c04651
ACS Omega 2024, 9, 4263−4276

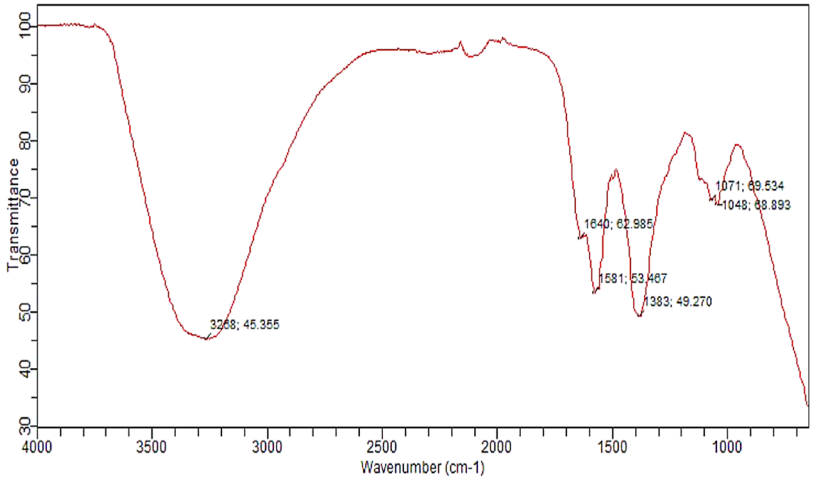


**Figure 2.** FTIR spectrum of OME.

and $q_0$ are the Langmuir constants determined from the slope and intercept of the plot of $\frac{1}{q_e}$ vs $\frac{1}{C_e}$, respectively.

*2.15.2. Freundlich Isotherm.* This assumes that the core sample comprises heterogeneous surfaces with different adsorption sites. This presumes that the quantity of the OME on the core sample relative to the concentration of the surfactant via an aqueous phase remains constant irrespective of the surfactant concentration. It also assumes that cations and anions are adsorbed onto the same surface simultaneously. The Freundlich isotherm is given by eq 7

$$q_e = K_f C_e^{1/n} \tag{7}$$

where $K_f$ and $1/n$ are the Freundlich constants.

*2.15.3. Temkin Isotherm.* This was used to investigate the indirect interaction between the natural surfactant and the core sample, especially for several experimental investigations as was the case in the current study. This isotherm illustrates that the larger the bulk or scoop, the lower the heat of adsorption. The Temkin isotherm is given by eq 8.

$$q_e = B \ln K_t + B \ln C_e \tag{8}$$

where $B$ = Temkin's constant and $K_t$ = equilibrium binding constant.

*2.15.4. Linear Isotherm.* This isotherm limits its consideration to a lower concentration range of the surfactant, whereas a higher surfactant concentration gives a nonlinear adsorption isotherm trend. The linear isotherm is illustrated by Henry equation as shown by eq 9

$$q_e = K_H C_e + C \tag{9}$$

where $K_H$ = linear isotherm constant ($L/m^2$) and $C$ = constant of proportionality.

**2.16. Adsorption Kinetics.** Kinetic evaluation of the adsorption process is vital in appraising the behavior of the OME in its interaction with the core sample. A change in surfactant concentration would indicate the amount of residence time required for the adsorption process to take place on the core sample, which could be investigated using various kinetic approaches. In the current study, formulations have been derived to illustrate the kinetic behavior of this liquid−solid system. Furthermore, it has been reported that the possible adsorption mechanism of such a system can be estimated through an adsorption kinetics study. To this end, the pseudo-first-order, pseudo-second-order, intraparticle diffusion, and Elovich models were used to evaluate the percentage of adsorption of the OME on the surface of the core sample. This was executed under ambient temperature (28 °C) over a 10 day (14,400 min) period.

*2.16.1. Pseudo-First-Order Model.* This model is expressed as seen in eq 10

$$\frac{dq_t}{dt} = K_1(q_e - q_t) \tag{10}$$

Integrating eq 11 is expressed in a linear form eq 11

$$\ln(q_e - q_t) = \ln(K_1 q_e) - K_1 t \tag{11}$$

where $K_1$ = pseudo-first-order rate constant ($min^{-1}$) and $q_e$ and $q_t$ = adsorption capacities of the core sample (mg/g) at equilibrium and time, $t$ (min), respectively.

*2.16.2. Pseudo-Second-Order Model.* The pseudo-second-order model is shown in eq 12 and is mainly used to predict the kinetic trend.

$$\frac{dq_t}{dt} = K_2(q_e - q_t)^2 \tag{12}$$

Integrating and rearranging eq 12 give a linear form most suitable for a solid−liquid system as shown in eq 13

$$\frac{t}{q_t} = \frac{1}{K_2 q_e^2} + \frac{t}{q_e} \tag{13}$$

where $K_2$ = pseudo-second-order rate constant (g/mg min) and $K_2$ and $q_{e,cal}$ can be determined from the intercepts and slope of the linear plot, respectively.

Also, the initial adsorption rate ($h$) and half adsorption time are given by eqs 14 and 15, respectively.

$$h = K_2 q_e^2 \tag{14}$$

$$t^{1/2} = 1/K_2 q_e \tag{15}$$

*2.16.3. Intraparticle Diffusion Model.* The intraparticle diffusion model is shown in eq 16 and describes the diffusion mechanism of the surfactant on the core sample.

$$q_t = K_i \times t^{1/2} \tag{16}$$



https://doi.org/10.1021/acsomega.3c04651
ACS Omega 2024, 9, 4263−4276

where $K_i$ = intraparticle diffusion model rate constant.

*2.16.4. Elovich Model.* The Elovich model is shown in eq 17, and it describes the chemisorption processes.

$$\frac{dq_t}{dt} = \alpha e^{-\beta q_t} \tag{17}$$

Assuming that $\beta\alpha t \gg 1$, eq 17 is transformed by applying the boundary conditions $q = 0$ at $t = 0$ and $q = q_t$ at $t = t$ which gives eq 18

$$\frac{1}{q_t} = \frac{\ln(\alpha\beta)}{\beta} + \frac{\ln(t)}{\beta} q_t \tag{18}$$

where $\alpha$ = initial adsorption rate (mg/g min) and $\beta$ = adsorption constant throughout the experiment (mg/g min).

## 3. RESULTS AND DISCUSSION

**3.1. FTIR Analysis of OME.** The FTIR spectrum of the aqueous extract of the orange mesocarp is shown in Figure 2. The band at 3288 $cm^{-1}$ is due to the O−H stretching vibration of phenol and sugar alcohol. The frequency of the band shows possible intermolecular hydrogen bonding. The band at 1640 $cm^{-1}$ is attributable to the presence of ketone groups (C═O) in the molecule. At 1581 $cm^{-1}$, a plane vibration was observed, which is indicative of the aromatic C═C groups present at this region. The C−O stretching vibration observed at bands 1071 and 1048 $cm^{-1}$ is indicative of the alcohol group. The spectrum indicates an extract composed of mainly keto-bearing phenolics and sugars which is consistent with rutin, a citrus flavonoid glycoside found in some vegetables and fruits. The structure of rutin is shown in Figure 3.

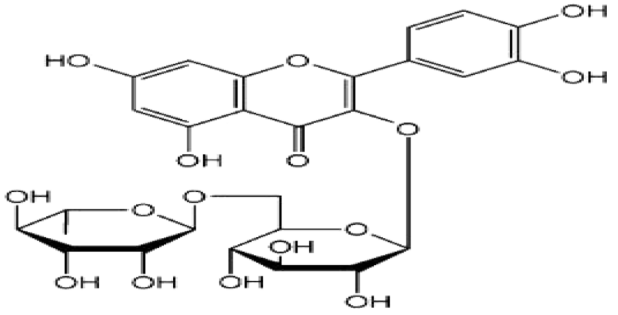


**Figure 3.** Chemical structure of rutin. Reprinted with permission from Mauludin, R.; Muller, R. H. Preparation and storage stability of rutin nanosuspensions, *J. Pharm. Invest.* **2013, 43,** 395−404. Springer Nature[53].

**3.2. Crude Oil Characterization.** From the characterization of the crude oil sample at ambient and reservoir temperatures as shown in (Table 2), the resultant value of the API gravity, 17.1° and 20.8°, at ambient and reservoir temperatures, respectively, indicates that it is a heavy crude as previously reported[38] with a corresponding API increase with temperature. Furthermore, an increase in temperature resulted in a decrease in the viscosity of the crude oil due to the reduction of the cohesive forces between the molecules in the oil. This corroborates the effect of temperature on the viscosity of crude oil.[39] The TAN for the crude oil sample was adjudged to be high.

Other physicochemical properties of the fluid which were measured at 25 and 80 °Care shown in Table 3. An inverse relationship was observed between the temperature, viscosity, and density of the brine and surfactant. At 80 °C, the resultant OME viscosity is 2.4 cP, while that of hard brine (1.02 cP) was slightly higher than the soft brine viscosity (0.85 cP). This is in line with the findings of Olayiwola and Dejam[40] that fluid viscosity is increased by the presence of divalent anions.

**Table 2. Parameters and Results of the Oil Sample**

| physical properties | values at 25°C | values at 80°C |
|---|---|---|
| density ($kg/m^3$) | 949 | 926 |
| specific gravity | 952 | 929 |
| API (deg) | 17.1 | |
| viscosity (mPa·s) | 89.8 | 9.7 |
| asphaltene (wt %) | 0.77 | |
| TAN (mg KOH/g) | 1.37 | |
| color | brownish black | |
| pH value | 6.2 | |

**Table 3. Physicochemical Properties of the Fluid**

| properties | distilled water | hard brine | soft brine | OME @ 1 g/L |
|---|---|---|---|---|
| (a) fluid properties at 25 °C temperature | | | | |
| density ($g/cm^3$) | 0.9952 | 1.0187 | 1.0171 | 1.0013 |
| SG | 0.9984 | 1.0218 | 1.0204 | 1.0045 |
| viscosity (cP) | 0.87 | 1.25 | 0.97 | 4.2 |
| (b) fluid properties at 80 °C temperature | | | | |
| density ($g/cm^3$) | 0.995 | 0.9923 | 0.9918 | 0.9672 |
| SG | 0.998 | 1.0142 | 1.0123 | 0.9891 |
| viscosity (cP) | 0.87 | 1.02 | 0.85 | 2.4 |

## 4. PHASE BEHAVIOR ANALYSIS

**4.1. pH Characterization.** The pH values of the OME in brine and distilled water indicate that the extract is highly alkaline and increases as the concentration of the extract increases (Figure 4). The pH values of most surfactants have been reported to be less than 7 with, sodium dodecyl sulfate (SDS), a synthetic surfactant that is often used during surfactant flooding, having a pH value of 6.5 at 1% concentration.[42] However, the high pH value obtained for the OME is largely due to the use of 1% sodium hydroxide solution during the extraction process. A pH of 12 was obtained with OME in distilled water solution, but the introduction of ions (NaCl) into the distilled water reduced the alkalinity, although a high pH of 11.7 was obtained with the introduction of divalent ions.

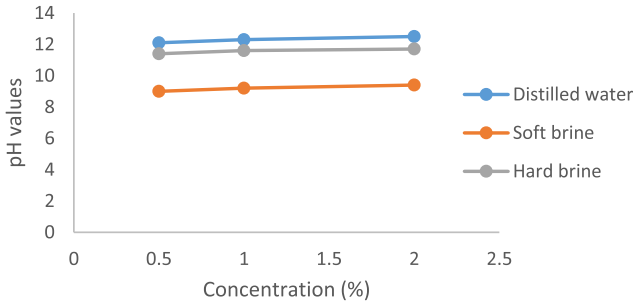


**Figure 4.** pH Values of OME.

**4.2. Compatibility Test.** Results of compatibility test on the OME at varying concentrations (0.5, 1.0, and 2.0%) in both brine samples presented limpid, consistent solutions at ambient temperature (25 °C) and under elevated temperatures



https://doi.org/10.1021/acsomega.3c04651
ACS Omega 2024, 9, 4263−4276

ranging from 30 to 80 °C (Figure 5). This is indicative of the high solubility and tolerance level of the OME for divalent ions

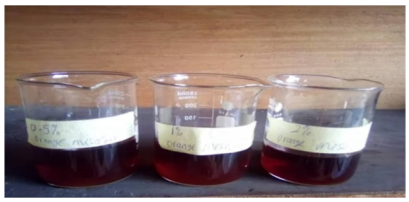

**Figure 5.** Compatibility test of OME in soft brine at 80 °C.

under elevated temperature. It can chelate divalent ions and as such can be used even in the presence of hard waters without the need to soften the water (brine).

**4.3. Critical Micelle Concentration.** Evaluating the electrical conductivity of the OME under varied concentrations, the CMC of the surfactant was obtained (Figure 6).

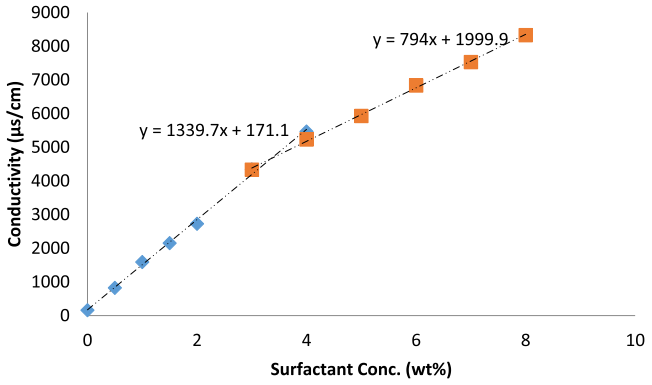


**Figure 6.** Conductivity vs concentration to determine the CMC of OME.

The point of inflection was estimated at 3.4 wt % concentration. The CMC value obtained in this study also corroborates that of similar green surfactants.[18] The relationship between CMC and IFT has been well established.[16,18,28,33] This underscores the report of Sheng[8] which stated that surfactant concentration above CMC will result in little or no change to the surface or IFT.

**4.4. Salinity Scan.** A constant volume for the natural surfactant was observed, while the brine salinity was varied. For both salinity cases (high and low), no phase separation was observed, while increase in pH resulted in a corresponding increase in the salinity of the soft brine (Figure 7). At salinities ranging from 0.5 to 3.5%, clear solutions were seen across the temperature range. Alkalinity is an important parameter in alkaline−surfactant (A−S) flooding because of its crucial role in altering rock wettability. Conversely, for hard brine, the pH of the solution decreased slightly as the brine salinity increased (11.7−10.8), implying that a hard brine salinity is inversely proportional to alkalinity, which is necessary for changing the rock wettability to obtain an ultralow IFT.[10]

**4.5. IFT Measurements.** The compositions of the two formulated brines considered include soft brine (NaCl, KCl) and hard brine (NaCl, KCl, $CaCl_2$, and $MgCl_2$). Considered alongside, this was the effect of the temperature on the IFT. Both brines produced lower IFT than that produced when distilled water was used (which had a high IFT value of 14.0 mN/m), suggesting the possible influence of the salt ions on

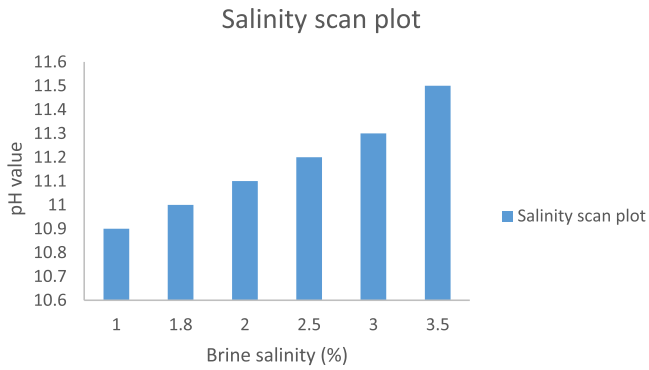


**Figure 7.** Plot showing alkalinity as a function of salinity.

the IFT (Table 4). The IFT value of surfactant concentration at CMC (3.4%) as well as a lower concentration of 3.0% was

**Table 4. Effect of the Brine Composition on IFT**

| composition | 3% OME + soft brine + oil | | 3% OME + hard brine + oil | |
|---|---|---|---|---|
| temp (°C) | 25 | 80 | 25 | 80 |
| IFT | 2.64 | 1.98 | 2.05 | 1.73 |

first determined, a resultant IFT value of 3.42 and 3.46 mN/m, respectively, was obtained. Surfactant concentration at 3.0% was chosen as a more cost-effective option. 3.0% surfactant concentration was added to both brines. In both brine cases, a reduction in IFT was observed with a corresponding increase in temperature. Thus, an IFT value of 2.64 and 1.98 mN/m was obtained for OME in soft brine at 25 and 80 °C, respectively, while OME in hard brine resulted in an IFT value of 2.05 and 1.73 mN/m at 25 and 80 °C, respectively. The results showed that OME is a good surfactant due to its ability to reduce the IFT between the brine and oil regardless of the temperature and brine composition.[43]

**4.6. Phase Separation.** Pipet test performed on the natural surfactant in soft brine at varied salinities with crude oil produced a middle phase microemulsion at ambient temperature (Figure 8), suggestive of an ultralow IFT. This is possible

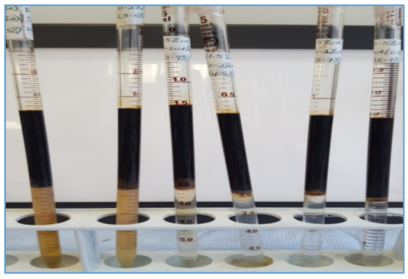

**Figure 8.** Phase separation of 3.0% OME in soft brine and crude oil at 25 °C.

due to the use of alkaline solution as the extraction solvent. Sheng[24] noted that a synergy between alkaline and surfactant chemicals is crucial in obtaining an ultralow IFT. At laboratory conditions, optimal salinity was estimated as 2.0%. With an increase in the temperature to 80 °C, samples were monitored for 16 days, a bicontinuous microemulsion was observed only in 3 wt % salinity, and salinities below 3% formed a type II microemulsion. This corroborates the reports of Healy et al.,[44] where it was discovered that temperature is directly propor-



https://doi.org/10.1021/acsomega.3c04651
ACS Omega 2024, 9, 4263−4276

tional to the optimal salinity of the aqueous system. A repeat test carried out in hard brine resulted in a bicontinuous microemulsion at varied temperatures (Figure 9). Solubilization ratio plot gave an optimal salinity value of 3.0% (Figure 10). This results also alludes to the fact that divalent ions increase the optimal salinity value of a brine solution.

**Figure 9.** Phase separation of 3.0% of the OME in hard brine and crude oil at 80 °C.

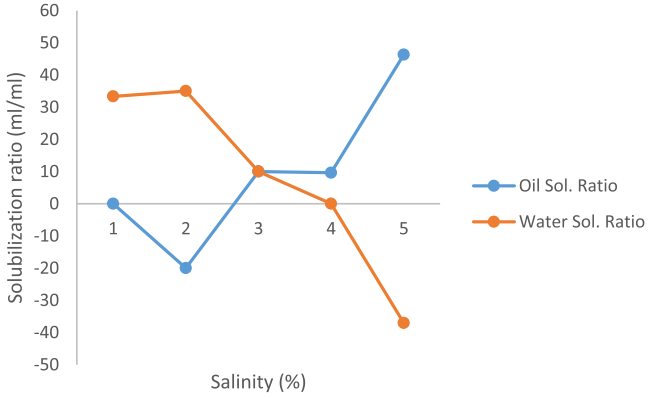


**Figure 10.** Solubilization plot of OME in hard brine at 80 °C.

**4.7. Calculated Properties of Core Plug.** Petrographic data of the well shows that the mineralogy of the core plug, which was analyzed using X-ray diffraction presents a graywacke sandstone with poorly sorted, angular, sand-sized grains, which are predominantly composed of quartz (>93%), feldspar (1%), minor amount of lithic fragments, and clay-fine matrix (<5%). The pore volume and porosity of the sandstone core were estimated as 15.3 $cm^3$ and 21%, respectively (Table 5). The porosity value (21%) falls within the range of porosity values for sandstones as reported.[41]

**4.8. Core Flooding.** This test was carried out using the extract as the surface-active agent at different concentrations of both formulated brines consecutively (starting with the soft brine) at 3.0% optimum salinity. In a bid to ascertain the relationship between surfactant concentration and oil recovery, surfactant concentrations at CMC and below CMC were adopted as 1.0, 2.0, and 3.0 wt %. A repeat surfactant injection was carried out using 3.0% hard brine. Fluid saturations, fluid volumes, and oil recovery efficiencies were measured and are presented in Tables 6 and 7.

**Table 5. Properties of the Core Sample**

| parameter | value |
|---|---|
| length (cm) | 5.8 |
| diameter (cm) | 4.0 |
| bulk volume ($cm^3$) | 73.0 |
| mass of unsaturated core (g) | 127.6 |
| mass of saturated core (g) | 143.2 |
| mass of brine (g) | 15.6 |
| density of brine ($g/cm^3$) | 1.02 |
| pore volume ($cm^3$) | 15.3 |
| porosity (%) | 21.0 |

It was observed that at an optimum brine salinity of 3.0%, secondary flooding with soft brine recovered more additional heavy oil compared to that of flooding with hard brine even though hard brine was more viscous than soft brine. This underpins the fact that salinity and divalent ions play a more vital role during surfactant flooding than that of viscosity. However, EOR using the natural surfactant, OME at 2 wt % with hard brine, resulted in an additional recovery of 44% OOIP as opposed to surfactant flooding with soft brine where an additional recovery of 29.1% OOIP was obtained (Figure 11a). A slightly higher recovery (45% OOIP and 29.2% OOIP) was obtained when flooding at surfactant CMC in hard and soft brine, respectively, thus validating the findings of Obuebite et al.[16] and Wojton et al.[15] which affirms the ability of natural surfactants to lower surface tension in the presence of divalent ions. It was also observed that the additional recovery obtained between 2 and 3 wt % was minimal (Figure 11a); this could be because of surfactant loss due to adsorption in the porous medium. Belhaj et al.[54] also reported that increasing the surfactant concentration increases surfactant adsorption. They noted that at concentration below CMC, "the charge in the electrical double layer controls the rate of adsorption"; however, there is a corresponding increase in the adsorption density as the surfactant concentration increases toward CMC.

Oil displacement analysis depicts the synergistic interaction of the natural surfactant with the alkaline solution (surfactant−enriched-alkaline system) which resulted in an ultralow IFT acting as the main recovery mechanism. The surfactant interacting with the trapped oil lowered the IFT and solubilized the oil, thereby boosting residual oil recovery.[45] A plot of pore volume injected (PVI) as a function of recovery factor (Figure 11b) showed an incremental oil recovery over an injection volume of 0.08% between 1PV and 2PV; however, a minimal decrease in oil recovery was observed as injection volume increased above 2PV. The significant higher oil recovery factor when flooding with hard brine can be related to the lower IFT value (1.73 mN/m) obtained using the OME and hard brine solution. The natural surfactant, OME, is a more effective surfactant due to its ability to chelate divalent ions, attain a low IFT, reduce residual oil, and recover heavy oil even under challenging conditions.

**4.9. Adsorption Study.** The adsorption−concentration plot of the natural surfactant is shown in Figure 12.

The surfactant concentration before and after the adsorption test on the core sample was evaluated through a conductivity test from where the equilibrium concentration was determined, while the adsorption was calculated using eq 5. Figure 12 indicates that at higher concentrations of the surfactant and as the vacant sites of the core sample are filled with the surfactant, the slope of the plot decreases. This implies that there is high affinity of the core sample for this natural surfactant at low concentration. At low concentration of the extract, adsorption will most likely occur by physisorption rather than chemisorption. This is because unlike chemisorption which requires strong bonds between the adsorbate and the


https://doi.org/10.1021/acsomega.3c04651
ACS Omega 2024, 9, 4263−4276

**Table 6. Calculated Values of Fluid Volumes**[a]

| parameter | flooding with OME in soft brine | | | flooding with OME in hard brine | | |
|---|---|---|---|---|---|---|
| | 1.0% conc. | 2.0% conc. | 3.0% conc. | 1.0% conc. | 2.0% conc. | 3.0% conc. |
| pore volume | 15.3 | 15.3 | 15.3 | 15.3 | 15.3 | 15.3 |
| original oil in place | 10.0 | 11.0 | 12.0 | 11.0 | 10.0 | 10.0 |
| brine effluent volume | 5.3 | 4.3 | 3.3 | 4.3 | 5.3 | 5.3 |
| brine recovery | 7.0 | 7.0 | 8.0 | 6.5 | 5.0 | 5.0 |
| residual oil volume after imbibition | 3.0 | 4.0 | 4.0 | 4.5 | 5.0 | 5.0 |
| EOR | 2.2 | 3.2 | 3.5 | 3.5 | 4.4 | 4.5 |
| residual oil after EOR (%) | 0.8 | 0.8 | 0.5 | 1.0 | 0.6 | 0.5 |
| total volume of oil recovered | 9.2 | 10.2 | 11.5 | 10 | 9.4 | 9.5 |

[a]All units are in mL.

**Table 7. Calculated Values of Fluid Saturation and Recovery Efficiency**[a]

| parameter | fluid saturation and recovery efficiency | | | | | |
|---|---|---|---|---|---|---|
| initial oil saturation ($S_{oi}$) | 65.4 | 71.9 | 78.4 | 71.9 | 65.4 | 65.4 |
| initial water saturation ($S_{wi}$) | 34.6 | 28.1 | 21.6 | 28.1 | 34.6 | 34.6 |
| primary and secondary recovery | 70.0 | 63.6 | 66.6 | 59.1 | 50.0 | 50.0 |
| residual oil saturation ($S_{or}$) | 30.0 | 36.4 | 33.4 | 40.9 | 50.0 | 50.0 |
| recovery factor (EOR) | 22.0 | 29.1 | 29.2 | 31.8 | 44.0 | 45.0 |
| critical oil saturation | 8.0 | 7.3 | 4.2 | 9.1 | 6.0 | 5.0 |
| total oil recovery | 92 | 92.7 | 95.8 | 90.9 | 94.0 | 95.0 |
| displacement efficiency after EOR | 73.3 | 80.0 | 87.5 | 77.8 | 88.0 | 90.0 |

[a]All values are in %.

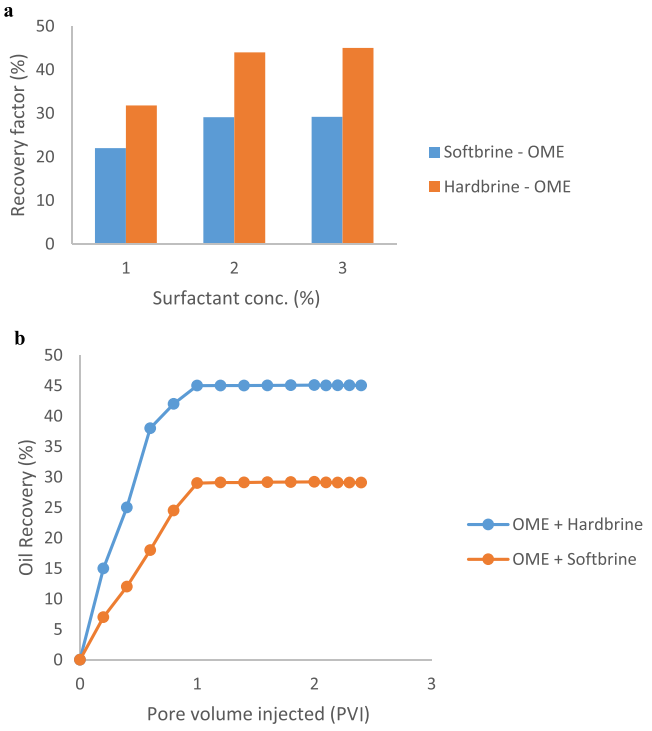


**Figure 11.** (a) Recovery factor of OME in soft and hard brine. (b) Plot of recovery factor vs pore volume injected.

adsorbent, in this study, the molecules of the OME must have been bonded with the core by weak van der Waals forces, thereby making it easier for the OME to be adsorbed by the core at low concentration. A similar pattern has earlier been

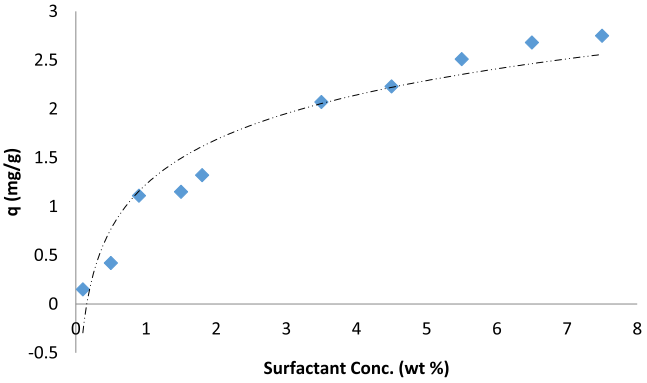


**Figure 12.** Adsorption vs concentration of the natural surfactant (OME).

reported for a natural surfactant obtained from the leaf extract of *Zyziphus spina-choursisti* (ZSC).[46,47] The effect of surfactant concentration on EOR operation could have both technical and economic implications because losses caused by adsorption pose a major challenge in surfactant flooding. According to Ahmadi and Shadizadeh,[47] adsorption of surfactants on rock surfaces may lead to a reduction of their concentrations in aqueous solutions, thereby rendering them ineffective for EOR operation.

**4.10. Adsorption Models.** The results obtained from the adsorption models are shown in Figures 13−16 and Table 8:

The Langmuir isotherm plot is shown in Figure 13.
The Freundlich isotherm plot is shown in Figure 14.
The Temkin isotherm plot is shown in Figure 15.
The linear isotherm plot is shown in Figure 16.

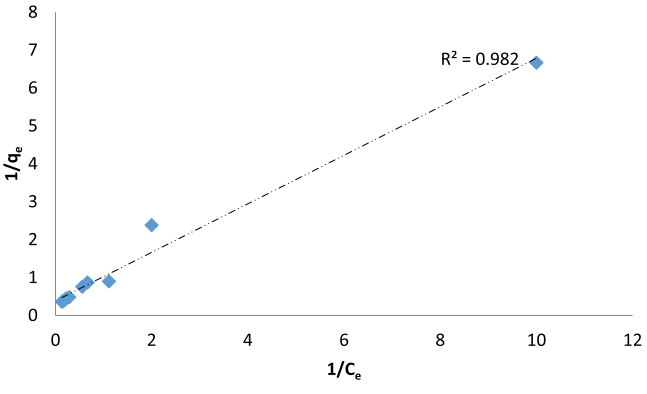


**Figure 13.** Langmuir adsorption model.



https://doi.org/10.1021/acsomega.3c04651
ACS Omega 2024, 9, 4263−4276

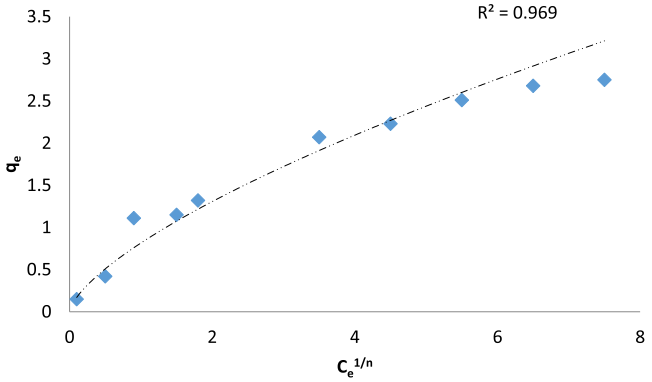


**Figure 14.** Freundlich adsorption model.

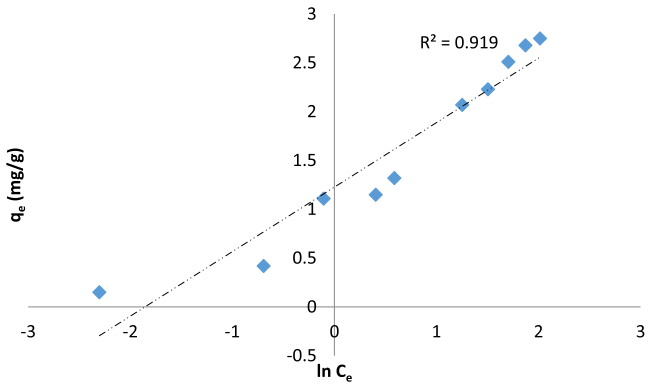


**Figure 15.** Temkin adsorption model.

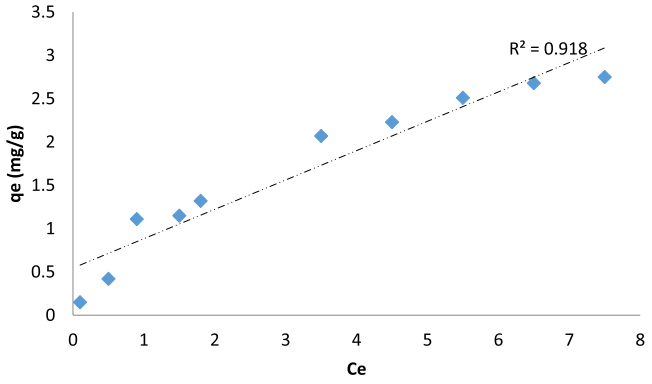


**Figure 16.** Linear adsorption model.

**Table 8. Fitted Adsorption Model Parameters for This Study**

| isotherm | model | $R^2$ | parameters |
|---|---|---|---|
| Langmuir | $1/q_e = 0.64(1/C_e) + 0.384$ | 0.982 | $q_0 = 2.604$; $K_{ad} = 1/0.64q_e$ |
| Freundlich | $q_e = 0.815C_e^{0.68}$ | 0.969 | $1/n = 0.68$; $K_f = 0.815$ |
| Temkin | $q_e = 0.660 \ln C_e + 1.226$ | 0.919 | $B = 0.660$; $K_t = 6.408$ |
| linear | $q_e = 0.338C_e + 0.544$ | 0.918 | $B = 0.544$; $K_H = 0.338$ |

From the results of the adsorption-fitted parameters from this study (Table 8), all the models gave good prediction of the adsorption trend of this natural surfactant on the core sample based on the correlation coefficient ($R^2$) values. However, with the highest $R^2$ value, the Langmuir isotherm gave the best prediction of this process. From the result, this model assumes that adsorption of the natural surfactant (OME) on the crushed core sample takes place on specific homogeneous sites, which when occupied by higher concentration of the surfactant cannot allow further adsorption on these sites. This gives further justification to the adsorption−concentration pattern in this study. Also, the high value of the Freundlich isotherm also indicates that the core sample could have different sites for adsorption, although the former accounts more for this process than the latter. The adsorption model parameters for other natural surfactants have also been reported.[47,48,50,51]

**4.11. Adsorption Kinetics.** As previously stated, this is an important parameter for the investigation of the adsorption pattern. Since it was observed that the adsorption of the natural surfactant was rapid before the attainment of equilibrium, it was therefore necessary to investigate the rate of the process. Moreover, the proper choice of kinetic approach is essential for the prediction of surfactant loss rate and for the right design of a surfactant-based EOR mechanism from the reservoir. The fitting of the experimental data using these models are presented in Figures 17−20. Also, Tables 9−12 show the fitted adsorption kinetic parameters using the pseudo-first-order, pseudo-second-order, intraparticle diffusion, and Elovich models, respectively, across different concentrations of the surfactant.

The plot of the pseudo-first-order kinetic model and the fitted kinetic parameters for this model from the experimental data of the natural surfactant and the core sample is shown in Figure 17a,b and Table 9 across different concentrations of the surfactant. The pseudo-first-order approach describes the role of adsorption capacity of the adsorbent (core sample) on the rate of the process. All surfactant concentrations considered in this study gave high correlation coefficient ($R^2$) values. This shows that the core sample used for this experimental study had a good adsorption capacity. The higher $R^2$ values at the low surfactant concentration range at 0.5 wt % (0.986) further corroborates the earlier findings from this study that the core sample has more affinity for the surfactant (OME) at this concentration, hence the faster rate of adsorption under this condition. This could have some implications in the EOR process because most of the surfactants could be adsorbed in the sandstone reservoir. Several studies have also highlighted the impact of high concentration of natural surfactants in the EOR process.[33,47]

The pseudo-second-order kinetic model, which is an indication of the kinetic trend of the entire adsorption process, adequately fitted the experimental data across all concentrations considered in this study as shown in Figure 18a,b and Table 10. Although other linear forms of the model exist, the suitability of the form employed in the current study for predicting the rate of liquid−solid system has been highlighted by Ahmadi and Shadizadeh[47] and Oduola and Okwonna.[52] The high correlation coefficient ($R^2$) value across all the concentrations considered also shows that these concentrations are favorable for the process. The highest $R^2$ values were obtained at 1 and 7 wt % concentrations of the natural surfactant at 0.998 and 0.997, respectively. Similarly, $R^2$ values of 0.982, 0.985, and 0.990 were obtained at 0.5, 1.5, and 6 wt % surfactant concentrations, respectively. Furthermore, with the pseudo-second-order kinetic model, estimation of the initial adsorption rate and half adsorption time can be made as it is able to account for the rate limiting step and considers as many


https://doi.org/10.1021/acsomega.3c04651
ACS Omega 2024, 9, 4263−4276

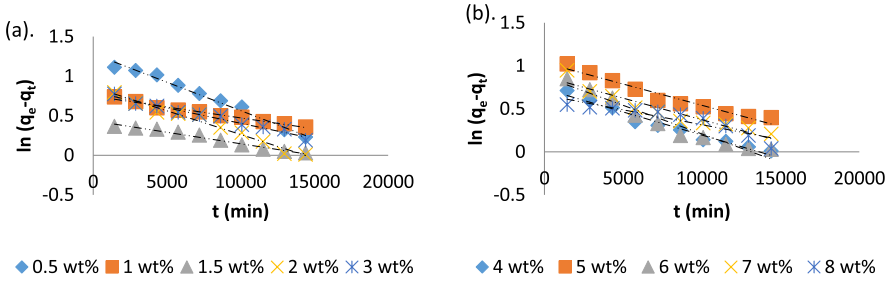


**Figure 17.** Pseudo-first-order kinetic model for (a) 0.5−3 wt % surfactant conc. (b) 4−8 wt % surfactant conc.

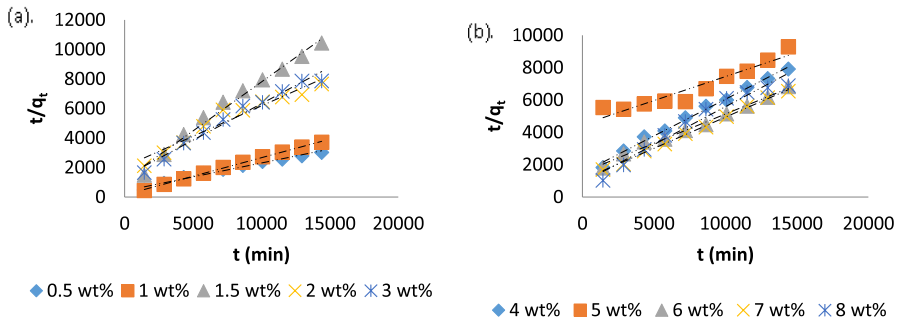


**Figure 18.** Pseudo-second-order kinetic model for (a) 0.5−3 wt % surfactant conc. (b) 4−8 wt % surfactant conc.

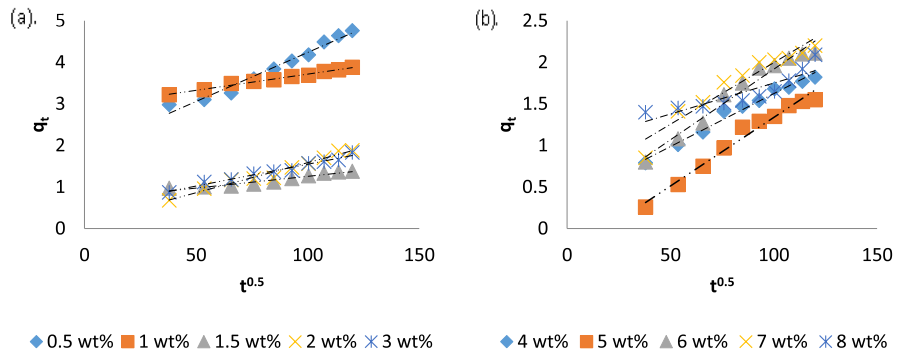


**Figure 19.** Intraparticle diffusion kinetic model for (a) 0.5−3 wt % surfactant conc. (b) 4−8 wt % surfactant conc.

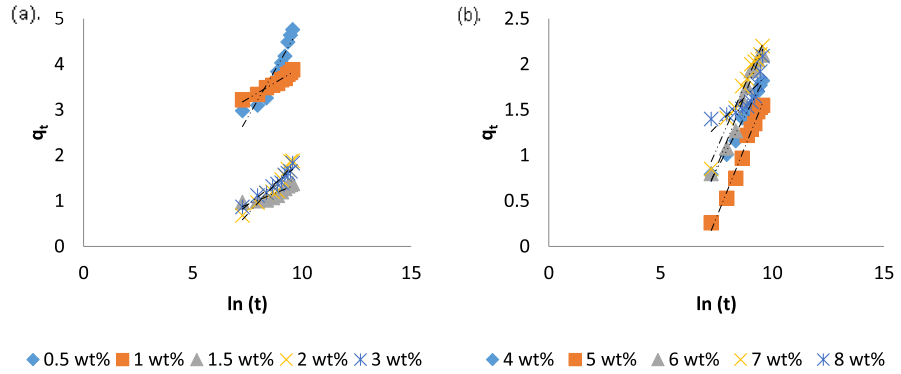


**Figure 20.** Elovich kinetic model for (a) 0.5−3 wt % surfactant conc. (b) 4−8 wt % surfactant conc.

adsorption sites as possible within the core sample and their capacities and as such best describes the entire process.[52]

The intraparticle diffusion kinetic model plots are shown in Figure 19a,b across the various concentrations considered, while their parameter estimates are shown in Table 11.

Figure 19a,b indicates the multilinear nature of the experimental data obtained in this study. It shows that the diffusion mechanism of the surfactant on the core sample obeys a multilinear behavior. This model describes the rate at which the natural surfactant diffuses toward the core sample.[52] The correlation coefficient ($R^2$) values in Table 11 also favor the low concentration range of the surfactant of 1 wt % (0.991) and as such their ease of migration through the sandstone reservoir. This is in agreement with previous models



https://doi.org/10.1021/acsomega.3c04651
ACS Omega 2024, 9, 4263−4276

**Table 9. Fitted Kinetic Adsorption Parameters Using the Pseudo-First-Order Model at Different Surfactant Concentrations**

| surfactant conc. (wt %) | model | $R^2$ |
|---|---|---|
| 0.5 | $\ln(q_e - q_t) = -7 \times 10^{-5}t + 1.281$ | 0.986 |
| 1 | $\ln(q_e - q_t) = -3 \times 10^{-5}t + 0.748$ | 0.980 |
| 1.5 | $\ln(q_e - q_t) = -3 \times 10^{-5}t + 0.435$ | 0.975 |
| 2 | $\ln(q_e - q_t) = -6 \times 10^{-5}t + 0.861$ | 0.973 |
| 3 | $\ln(q_e - q_t) = -4 \times 10^{-5}t + 0.796$ | 0.969 |
| 4 | $\ln(q_e - q_t) = -5 \times 10^{-5}t + 0.731$ | 0.967 |
| 5 | $\ln(q_e - q_t) = -5 \times 10^{-5}t + 1.035$ | 0.954 |
| 6 | $\ln(q_e - q_t) = -7 \times 10^{-5}t + 0.872$ | 0.944 |
| 7 | $\ln(q_e - q_t) = -5 \times 10^{-5}t + 0.874$ | 0.906 |
| 8 | $\ln(q_e - q_t) = -3 \times 10^{-5}t + 0.661$ | 0.845 |

**Table 10. Fitted Kinetic Adsorption Parameters Using the Pseudo-Second-Order Model at Different Surfactant Concentrations**

| surfactant conc. (wt %) | model | $R^2$ |
|---|---|---|
| 0.5 | $t/q_t = 0.188t + 420.7$ | 0.982 |
| 1 | $t/q_t = 0.251t + 149.5$ | 0.998 |
| 1.5 | $t/q_t = 0.663t + 1162$ | 0.985 |
| 2 | $t/q_t = 0.411t + 2062$ | 0.943 |
| 3 | $t/q_t = 0.494t + 1382$ | 0.975 |
| 4 | $t/q_t = 0.453t + 1506$ | 0.992 |
| 5 | $t/q_t = 0.296t + 4477$ | 0.913 |
| 6 | $t/q_t = 0.361t + 1516$ | 0.990 |
| 7 | $t/q_t = 0.386t + 1078$ | 0.997 |
| 8 | $t/q_t = 0.468t + 896.2$ | 0.956 |

**Table 11. Fitted Kinetic Adsorption Parameters Using the Intraparticle Diffusion Model at Different Surfactant Concentrations**

| surfactant conc. (wt %) | model | $R^2$ |
|---|---|---|
| 0.5 | $q_t = 0.023t^{0.5} + 1.877$ | 0.973 |
| 1 | $q_t = 0.007t^{0.5} + 2.935$ | 0.991 |
| 1.5 | $q_t = 0.005t^{0.5} + 0.690$ | 0.939 |
| 2 | $q_t = 0.014t^{0.5} + 0.137$ | 0.971 |
| 3 | $q_t = 0.010t^{0.5} + 0.497$ | 0.975 |
| 4 | $q_t = 0.012t^{0.5} + 0.349$ | 0.980 |
| 5 | $q_t = 0.016t^{0.5} - 0.313$ | 0.975 |
| 6 | $q_t = 0.017t^{0.5} + 0.217$ | 0.962 |
| 7 | $q_t = 0.014t^{0.5} + 0.513$ | 0.926 |
| 8 | $q_t = 0.007t^{0.5} + 1.005$ | 0.796 |

**Table 12. Fitted Kinetic Adsorption Parameters Using the Elovich Model at Different Surfactant Concentrations**

| surfactant conc. (wt %) | model | $R^2$ |
|---|---|---|
| 0.5 | $q_t = 0.831 \ln(t) - 3.416$ | 0.899 |
| 1 | $q_t = 0.283 \ln(t) - 1.114$ | 0.970 |
| 1.5 | $q_t = 0.196 \ln(t) - 0.553$ | 0.846 |
| 2 | $q_t = 0.519 \ln(t) - 3.191$ | 0.931 |
| 3 | $q_t = 0.379 \ln(t) - 1.936$ | 0.945 |
| 4 | $q_t = 0.468 \ln(t) - 2.675$ | 0.984 |
| 5 | $q_t = 0.607 \ln(t) - 4.241$ | 0.983 |
| 6 | $q_t = 0.627 \ln(t) - 3.847$ | 0.977 |
| 7 | $q_t = 0.559 \ln(t) - 3.138$ | 0.981 |
| 8 | $q_t = 0.250 \ln(t) - 0.562$ | 0.672 |

considered in this study and therefore gives a stronger indication that low concentration of the natural surfactant would ease their adsorption on rock surfaces during surfactant flooding and may lead to a reduction of their concentrations through the aqueous solution which reduces their effectiveness for EOR operation.

The Elovich model has been used to illustrate the kinetics of the chemisorption process of gases to solids. Considering Figure 20a,b, adsorption at lower concentration of the natural surfactant (0.5 and 1 wt %) per time was higher than what was obtained at higher concentrations (1.5−8 wt %). Again, this may not be unconnected to their ease of mobility toward the adsorbent as severally highlighted in the current study.

Elovich model also describes the adsorption process of the surfactant on the core sample adequately across all the concentrations considered. Increase in concentration gradient through the experimental process also had an impact on the process and the data fit into the model, and this corroborates the result of previous studies on this.[47,49]

Generally, the adsorption rate from this study highlights the effect of contact time on the adsorption of the natural surfactant in sandstone reservoirs during EOR operation using surfactant flooding. Across all concentrations (0.1−8 wt %) considered, a rapid decline was observed within the first 3 days (4320 min) of the study after which the process became much slower. This is attributable to the saturation of the surface area of the core sample at the initial phase, leading to a much slower process of pore diffusion of the surfactant molecules into the bulk surfaces of the core sample in the final phase of the experiment.

## 5. CONCLUSIONS

The capability of OME as a natural surfactant for the EOR processes was experimentally investigated. The compatibility of the natural surfactant (OME) in brine solution indicates that it is soluble and highly tolerant of divalent ions even under reservoir conditions of 100 °C, and it is highly controlled by pH and salinity. The natural surfactant−brine solution produced a bicontinuous microemulsion, which was enhanced by the alkaline nature of the surfactant system, implying that an ultralow IFT required to effectively enhance oil recovery through surfactant flooding was achieved. Core flooding analysis showed that OME achieved an improved recovery of the OME improved by 44% in divalent-ion-rich brine, in contrast to recovery using brine devoid of divalents (29.1%). Surfactant adsorption mechanism modeling showed that the Langmuir isotherm gave the highest correlation coefficient ($R^2$ = 0.982) relative to Freundlich, Temkin, and linear isotherm models, which suggests that adsorption of the surfactant (OME) on the crushed core sample took place on specific homogeneous sites, which when occupied by higher concentration of the surfactant cannot allow further adsorption on these sites. Effective flooding may not be achieved at low concentrations but will likely require a surfactant concentration equivalent to CMC (3.4%). Adsorption kinetics was modeled using pseudo-first-order, pseudo-second order, intraparticle diffusion, and Elovich models. The availability of OME as a cheap renewable resource easily obtainable from waste biomass is economically advantageous because higher concentrations will not be cost-prohibitive compared to conventional surfactants. Overall, orange mesocarp extract was effective as a natural surfactant for chemically enhanced oil recovery. The results support recent findings from other related research and



https://doi.org/10.1021/acsomega.3c04651
ACS Omega 2024, 9, 4263−4276

highlight the potential of natural biomass-based surfactants for EOR applications. Investigation of the long-term thermal and chemical stability of the OME and processes for green chemical derivatizations toward enhancing its surface-active properties for EOR is an area for future work.

## AUTHOR INFORMATION


### Corresponding Author

**Amalate Ann Obuebite** − *Department of Petroleum Engineering, Niger Delta University, Wilberforce Island PMB 071 Bayelsa State, Nigeria;* orcid.org/0000-0002-3917-9138; Email: amalateobuebite@ndu.edu.ng

### Authors

**Obumneme Onyeka Okwonna** − *Department of Chemical Engineering, University of Port Harcourt, Port Harcourt PMB 5323 Rivers State, Nigeria*

**William Iheanyi Eke** − *Department of Pure & Industrial Chemistry, University of Port Harcourt, Port Harcourt PMB 5323 Rivers State, Nigeria*

**Onyewuchi Akaranta** − *Department of Pure & Industrial Chemistry, University of Port Harcourt, Port Harcourt PMB 5323 Rivers State, Nigeria*

Complete contact information is available at: https://pubs.acs.org/10.1021/acsomega.3c04651


### Notes

The authors declare no competing financial interest.

## ACKNOWLEDGMENTS

This work was funded by the icipe-World Bank Financing Agreement no. D347-3A and World Bank-Korea Trust Fund agreement no TF0A8639 for the PASET Regional Scholarship and Innovation Fund (grant no: RSIF/RA/013).

## REFERENCES


(1) IRENA. *Global Energy Transformation, A Roadmap to 2050*; International Renewable Energy Agency: Abu Dhabi, 2018. www.irena.org/publications.

(2) Adeniyi, A. Surfactant selections criteria for Enhanced Oil Recovery in High Temperature and High Salinity Environment. *SPE J.* **2015**, *178404*, 2−3.

(3) Healy, R.; Reed, R. Immiscible microemulsion flooding. *SPE J.* **1977**, *17*, 129−139.

(4) Marhaendrajana, T.; Fauzi, I.; Buchari, A.; Wardhana, A.; Hasibuan, R. P. A successful small, scaled field testing of surfactant flooding in a waxy oil reservoir, Tanjing field, Indonesia-A case study. *4th International Conference on Petroleum Engineering*, London, UK, 2016.

(5) Rilian, N. A.; Sumestry, M.; Wahyuningsih, W. Surfactant Stimulation to Increase Reserves in Carbonate Reservoir A Case Study of Semoga Field. *SPE EUROPEC/EAGE Annual Conference and Exhibition*, Barcelona, Spain, 2010.

(6) Abbas, A. H.; Elhag, H. H.; Sulaiman, W. R. W.; Gbadamosi, A.; Pourafshary, P.; Ebrahimi, S. S.; Alqohaly, O. Y.; Agi, A. Modelling of continuous surfactant flooding application for marginal oilfields: a case study of Bentiu reservoir. *J. Pet. Explor. Prod. Technol.* **2021**, *11*, 989−1006.

(7) Chen, H. L.; Lucas, L. R.; Nogaret, L. A. D.; Yang, H. D.; Kenyon, D. E. Laboratory monitoring of surfactant imbibition with computerized tomography. *SPE Reservoir Eval. Eng.* **2001**, *4*, 16−25.

(8) Sheng, J. *Modern Chemical Enhanced Oil Recovery; Theory and Practice*; Gulf Professional Publishing, 2011; pp 239−260.

(9) Rudin, J.; Wasan, D. Mechanisms for Lowering of Interfacial Tension in Alkali/Acidic Oil Systems: Effect of Added Surfactant. *Ind. Eng. Chem. Res.* **1992**, *31*, 1899−1906.

(10) Liu, S.; Zhang, D.; Yan, W.; Puerto, M.; Hirasaki, G.; Miller, C. Favorable Attributes of Alkaline-Surfactant-Polymer Flooding. *SPE J.* **2008**, *13*, 5−16.

(11) Tabary, R.; Bazin, B.; Douarche, F.; Moreau, P.; Oukhemanou-Destremaut, F. Surfactant Flooding in Challenging Conditions: Towards Hard Brines and High Temperatures. *SPE J.* **2013**, *164359*, 2.

(12) Liu, S. Alkaline Surfactant Polymer Enhanced Oil Recovery Process. Ph.D. Dissertation, Rice University, Houston, 2007.

(13) Obuebite, A. A.; Okwonna, O. O. Performance Evaluation of Synthetic and Natural-Based Surfactants for Chemical Enhanced Oil Recovery. *J. Eng. Res. Rep.* **2022**, *22* (7), 1−11.

(14) Nowrouzi, I.; Mohammadi, A. H.; Manshad, A. K. Preliminary evaluation of a natural surfactant extracted from Myrtus communis plant for enhancing oil recovery from carbonate oil reservoirs. *J. Pet. Explor. Prod. Technol.* **2022**, *12*, 783−792.

(15) Wojton, P.; Szaniawska, M.; Holysz, L.; Miller, R.; Szcześ, A. Surface Activity of Natural Surfactants Extracted from Sapindusmukorossi and Sapindustrifoliatus soap nuts. *J. Colloid Interface Sci.* **2021**, *5* (1), 7.

(16) Obuebite, A.; Onyekonwu, M.; Akaranta, O.; Ubani, C.; Uzoho, C. An Experimental Approach to Low cost, High-performance Surfactant Flooding. *Sci. Afr.* **2020**, *8*, e00361−e02276.

(17) Cu, U.; Onyekonwu, M. O.; Akaranta, O. Chemical Flooding Enhanced Oil Recovery Using Local Alkali- Surfactant-Polymer. *Int. J. Innov. Res.* **2019**, *7* (1), 16−24.

(18) Ahmadi, M. A.; Shadizadeh, S. R. Spotlight on the New Natural Surfactant Flooding in Carbonate Rock Samples in Low Salinity Condition. *Sci. Rep.* **2018**, *8*, 10985.

(19) Akpoturi, P.; Ofesi, S. F. Enhanced Oil Recovery using local alkaline. *Niger. J. Technol.* **2017**, *36* (2), 515−522.

(20) Ogolo, N. A.; Ogiriki, S. O.; Onyiri, V. I.; Nwosu, T. C.; Onyekonwu, M. O. Performance of foreign and local agents for enhanced oil recovery of Nigerian crude. *SPE Nigeria Annual International Conference and Exhibition*, 2015; p 178305.

(21) Ojukwu, C.; Onyekonwu, M. O.; Ogolo, N. A.; Ubani, C. Alkaline Surfactant Polymer (Local) Enhanced Oil Recovery: An Experimental Approach. *SPE J.* **2013**, *167529*, 2−5.

(22) Chen, Y.; Yang, C.; Chang, M.; Ciou, Y.; Huang, Y. Foam Properties and Detergent Abilities of the Saponins from Camellia oleifera. *Int. J. Mol. Sci.* **2010**, *11* (11), 4417−4425.

(23) Rai, S.; Acharya-Siwakoti, E.; Kafle, A.; Devkota, H.; Bhattarai, A. Plant-Derived Saponins: A Review of their Surfactant Properties and Applications. *Science* **2021**, *3* (4), 44.

(24) Sheng, J. A Comprehensive Review of Alkaline-Surfactant-Polymer (ASP) Flooding. *SPE J.* **2013**, *9*, 4−10.

(25) Biesaga, M. Influence of extraction methods on stability of flavonoids. *J. Chromatogr. A* **2011**, *1218* (18), 2505−2512.

(26) Panche, A. N.; Diwan, A. D.; Chandra, S. R. Flavonoids: an overview. *J. Nutr. Sci.* **2016**, *5*, No. e47.

(27) Di Mattia, C. D.; Sacchetti, G.; Mastrocola, D.; Sarker, D. K.; Pittia, P. Surface properties of phenolic compounds and their influence on the dispersion degree and oxidative stability of olive oil O/W emulsions. *Food Hydrocolloids* **2010**, *24* (6−7), 652−658.

(28) Obuebite, A. A.; Eke, W. I.; Udoh, T. Evaluation of modified cashew nutshell liquid as natural surfactants for chemical flooding in sandstone oil reservoirs. *J. Eng. Appl. Sci.* **2022**, *69*, 114.

(29) Yang, D.; Wang, X.; Lee, J. H. Effects of flavonoids on physical and oxidative stability of soybean oil O/W emulsions. *Food Sci. Biotechnol.* **2015**, *24*, 851−858.

(30) Akaranta, O.; Osuji, L. Carboxymethylation of orange mesocarp cellulose and its utilization in drilling mud formulation. *Cellul. Chem. Technol.* **1997**, *31*, 193−198.

(31) Ibezim-Ezeani, M. U.; Okoye, F. A.; Akaranta, O. Studies on the Ion Exchange Properties of Modified and Unmodified Orange

Mesocarp Extract in Aqueous solution. *Int. Arch. Appl. Sci. Technol.* **2010**, *1* (1), 33−40.
(32) Luo, Z.; Murray, B. S.; Ross, A. L.; Povey, M. J.; Morgan, M. R.; Day, A. J. Effects of pH on the ability of flavonoids to act as Pickering emulsion stabilizers. *Colloids Surf., B* **2012**, *92*, 84−90.
(33) Obuebite, A.; Onyekonwu, M.; Akaranta, O.; Ubani, C. Phase behaviour of local alkaline and surfactants during flooding. *SPE J.* **2019**, *6*, SPE-198772-MS.
(34) Bachari, Z.; Isari, A. A.; Mahmoudi, H.; Moradi, S.; Mahvelati, E. H. Application of Natural Surfactants for Enhanced Oil Recovery − Critical Review. *IOP Conf. Ser. Earth Environ. Sci.* **2019**, *221*, 012039.
(35) Russo, C.; Maugeri, A.; Lombardo, G. E.; Musumeci, L.; Barreca, D.; Rapisarda, A.; Cirmi, S.; Navarra, M. The second life of citrus fruit waste: A valuable source of Bioactive compounds. *Molcules* **2021**, *26*, 5991.
(36) Oikeh, E. I.; Oriakhi, K.; Omoregie, E. S. Proximate Analysis and Phytochemical Screening of Citrus sinensis Fruit Wastes. *Bioscientist* **2013**, *1* (2), 164−170.
(37) Bolaji, T. A.; Oti, M. N.; Onyekonwu, M. O.; Bamidele, T.; Osuagwu, M.; Chiejina, L.; Elendu, P. Preliminary geochemical characterization of saline formation water from Miocene reservoirs, offshore Niger Delta. *Heliyon* **2021**, *7* (2), No. e06281.
(38) Soliman, E. Flow of Heavy oils at Low Temperatures: Potential Challenges and Solutions. *Processing of Heavy Crude Oils-Challenges and Opportunities*; Books on Demand, 2019.
(39) Santos, I. C. V. M.; Oliveira, P. F.; Mansur, C. R. E. Factors that affect crude oil viscosity and techniques to reduce it: A review. *Braz. J. Pet. Gas* **2017**, *11* (2), 115−130.
(40) Olayiwola, S. O.; Dejam, M. The impact of monovalent and divalent ions on the viscosity of a solution with silica nanoparticles. *Annual Conference of the APS Division of Fluid Dynamics*, WA, 2019, Vol. *72*.
(41) Guo, H.; Li, Y.; Wang, F.; Yu, Z.; Chen, Z.; Wang, Y.; Gao, X. ASP Flooding: Theory and Practice Progress in China. *J. Chem.* **2017**, *2017*, 1−18.
(42) Makowska, J.; Wyrzykowski, D.; Pilarski, B.; Chmurzyński, L. Thermodynamics of sodium dodecyl sulphate (SDS) micellization in the presence of some biologically relevant pH buffers. *J. Therm. Anal. Calorim.* **2015**, *121*, 257−261.
(43) Isehunmwa, S. O.; Olubukola, O. Interfacial tension of crude oil-brine systems in the Niger Delta. *Int. J. Recent Res. Appl. Stud.* **2012**, *10* (3), 460.
(44) Healy, R.; Reed, R.; Stenmark, D. Multiphase microemulsion systems. *SPE J.* **1976**, *16*, 147−160.
(45) Alpandi, A. H.; Inasyah, F. A.; Sidek, A.; Husin, H.; Junin, R.; Jaafar, M. Z. Critical micelle concentration, interfacial tension and wettability alteration study on the surface of paraffin oil-wet sandstone using saponin. *IOP Conf. Ser. Mater. Sci. Eng.* **2021**, *1153*, 012018.
(46) Ahmadi, M. A.; Shadizadeh, S. Experimental and Theoretical Study of a New Plant Derived Surfactant adsorption on Quartz Surface: Kinetic and Isotherm Methods. *J. Dispersion Sci. Technol.* **2015**, *36* (3), 441−452.
(47) Ahmadi, M. A.; Shadizadeh, S. Experimental investigation of a natural surfactant adsorption on shale-sandstone reservoir rocks: Static and dynamic conditions. *J. Fuel* **2015**, *159*, 15−26.
(48) Ahmadi, M. A.; Zendehboudi, S.; Shafiei, A.; James, L. Nonionic Surfactant for Enhanced Oil Recovery from Carbonates: Adsorption Kinetics and Equilibrium. *J. Ind. Eng. Chem. Res.* **2012**, *51* (29), 9894−9905.
(49) Ahmadi, M. A.; Shadizadeh, S. R. Experimental investigation of adsorption of a new non-ionic surfactant on carbonate minerals. *J. Fuel* **2013**, *104*, 462−467.
(50) Ahmadi, M. A.; Shadizadeh, S. R. Adsorption of novel non-ionic surfactant and particles mixture in carbonates: enhanced oil recovery implication. *Energy Fuel.* **2012**, *26*, 4655−4663.
(51) Zendehboudi, S.; Ahmadi, M. A.; Rajabzadeh, A. R.; Mahinpey, N.; Chatzis, I. Experimental study on adsorption of a new surfactant onto carbonate reservoir samples-application to EOR. *Can. J. Chem. Eng.* **2013**, *91* (8), 1439−1449.
(52) Oduola, M. K.; Okwonna, O. O. Kinetic Modelling of the Adsorption Treatment of Waste Lubricating Oil using Activated Ukpor Clay (Bentonite). *Int. J. Eng. Res. Sci.* **2016**, *2* (5), 113−123.
(53) Mauludin, R.; Muller, R. H. Preparation and storage stability of rutin nano suspensions. *J. Pharm. Invest.* **2013**, *43*, 395−404.
(54) Belhaj, A. F.; Elraies, K. A.; Mahmood, S. M.; Zulkifli, N. N.; Akbari, S.; Hussien, O. S. The effect of surfactant concentration, salinity, temperature, and pH on surfactant adsorption for chemical enhanced oil recovery: a review. *J. Pet. Explor. Prod. Technol.* **2020**, *10*, 125−137.


https://doi.org/10.1021/acsomega.3c04651
*ACS Omega* 2024, 9, 4263−4276